Thermodynamic Properties of QCD using the PNJL Model with Two Light Flavors

A Thesis Submitted
in Partial Fulfilment of the Requirements
for the Degree of

MASTER OF SCIENCE

by

MUBASHIR M

to the

School of Physical Sciences

National Institute of Science Education and Research

Bhubaneswar

May 14, 2024

DEDICATION

to my parents

DECLARATION

I hereby declare that I am the sole author of this thesis in partial fulfilment of the requirements for a postgraduate degree from the National Institute of Science Education and Research (NISER). I authorize NISER to lend this thesis to other institutions or individuals for the purpose of scholarly research.

Mubashir M
Date:

The thesis work reported in the thesis entitled Thermodynamic Properties of QCD using the PNJL Model with Two Light Flavors was carried out under my supervision, in the School of Physical Science at NISER, Bhubaneswar, India.

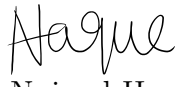

Dr. Najmul Haque
School Of Physical Science
Date: 14/05/2024

ACKNOWLEDGEMENTS

First and foremost, I would like to express my sincere gratitude to my supervisor, Dr. Najmul Haque, for his invaluable guidance and support throughout this MSc thesis project. His expertise in the field, insightful feedback, and unwavering encouragement were instrumental in shaping this work. I am particularly grateful for his patience during the challenging moments and his willingness to share his knowledge. I would also like to extend my thanks to Dr.Jobin Sabastian for his support and willingness to address my doubts.

finally, I would also like to thank my family and friends for their unwavering support and encouragement throughout my master's program. Their belief in me helped me persevere during difficult times.

ABSTRACT

This work investigates the thermodynamic properties of Quantum Chromodynamics (QCD) at finite temperature and quark chemical potential using the Polyakov Nambu-Jona-Lasinio (PNJL) model with two light quark flavours. This model incorporates both chiral symmetry breaking and deconfinement characteristics.

We numerically solve the PNJL potential under minimization conditions to obtain temperature-dependent mean fields. Subsequently, the crossover temperature is obtained to be 227 MeV. These results are then employed to calculate pressure, energy density, specific heat, speed of sound, and the conformal measure. Our findings are consistent with the observations in Mukherjee et al., 2006[23]. Additionally, we calculate the calculated pressure at finite chemical potential is used to obtain the Taylor series expansion coefficients of pressure around zero quark chemical potential.

Contents

1 Introduction **1**

2 PNJL Model For Two Flavor Quarks **3**
2.1 Polyakov Loop And Effective Potential In Pure Gauge Sector 4
2.2 Nambu Jona-Lasinio model 7
2.2.1 Two flavours NJL model in vacuum 7
2.2.2 parameter fixing 8
2.3 Coupling between quarks and the gauge sector 9

3 Formalism **11**
3.1 The Mean Fields And Cross Over Temperature 11
3.2 Taylor expansion of pressure 12
3.2.1 C_V, v_s^2, and $\mathcal{C}$ 13

4 Results **14**
4.1 Numerical Solution for the mean fields in finite temperature and zero chemical potential 14
4.2 Taylor expansion of pressure 16
4.3 C_V, v_s^2, and $\mathcal{C}$ 20

5 Summary and Conclusions **23**
5.1 Future Prospects 24

Appendix A Chiral Symmetry Breaking **28**

List of Figures

2.1 Scaled Polyakov loop effective potential $\frac{\mathcal{U}(\Phi,\bar{\Phi};T)}{T^4}$ as a function of for two values of temperature T, taking $\phi = \bar{\phi}$ 6

4.1 (a): scaled chiral condensate and Polyakov loop Φ as functions of temperature at zero chemical potential. (b): plots of $\partial\sigma(T)/\partial T$ and $\partial\Phi(T)/\partial T$. 15

4.2 The numerical Solution of (3.1) by taking $T_0 = 190MeV$. (a): scaled chiral condensate and Polyakov loop Φ as functions of temperature at zero chemical potential. (b): plots of $\partial\sigma(T)/\partial T$ and $\partial\Phi(T)/\partial T$. . . . 16

4.3 pressure scaled with the Stefan-Boltzmann pressure as a function of temperature in the PNJL model, at $\mu = 0$. The arrow on the right indicates the ideal gas value. 17

4.4 The QNS as a function of T/T_c. 18

4.5 The c4 as a function of T/T_c. 18

4.6 The c_6 as a function of T/T_c. 19

4.7 The c_8 as a function of T/T_c from the PNJL model 19

4.8 C_V/T^3 and $4\epsilon/T^4$ as a function of T/T_c. The dashed line on the right shows the ideal gas value. 20

4.9 Squared velocity of sound v_s^2 and conformal measure $\mathcal{C} = \Delta/\epsilon$ as a function of T/T_c . The dashed line on the right shows the ideal gas value for v_s^2. For comparison with v_s^2 we also plot the ratio P/ϵ 21

List of Tables

2.1 Parameter for the effective potential(2.5) in the pure gauge sector. . . 6
2.2 Parameter set used in the NJL model part of the effective Lagrangian (2.8), and the resulting physical quantities. we obtain a constituent quark mass $m = 325$MeV. 8

Chapter 1

Introduction

The study of strongly interacting matter at non-zero baryon density and high temperature holds immense significance across a broad spectrum of physicists. A comprehensive understanding of the multifaceted nature of strongly interacting matter, particularly the dynamics of colour deconfinement, promises insights into a variety of astrophysical (such as neutron stars, supernovae etc..) and cosmological phenomena[3, 20]. To probe such extreme conditions, accelerators such as those at CERN, Geneva[9], and RHIC, Brookhaven[10], have been built to collide beams of heavy nuclei at relativistic energies, effectively recreating matter under these extreme conditions.

The primary objective of the heavy-ion physics program lies in unravelling and comprehending phenomena such as the emergence of macroscopic collective behaviours and their influence on the evolution of strongly interacting systems. The analysis of data obtained from these experiments[5] necessitates a profound understanding of Quantum Chromodynamics (QCD). Vital thermodynamic properties, including the equation of state (EOS) and various transport coefficients, are indispensable in deciphering the intricate dynamics of these systems.

Quantum chromodynamics (QCD), the fundamental theory of strong interactions, provides a rich framework for understanding the behaviour of quarks and gluons[2]. However, the complexity of QCD makes direct calculations difficult, especially in the non-perturbative regime relevant to phenomena like confinement and the formation of

hadrons[21]. Effective field theories (EFTs) offer a powerful approach to tackle these challenges by focusing on the relevant degrees of freedom at specific energy scales[1].

The Polyakov-Nambu-Jona-Lasinio (PNJL) model emerges as a valuable EFT for these investigations[25]. It incorporates aspects of chiral symmetry breaking and deconfinement[14], allowing us to explore the complex interplay of quarks and gluons under various conditions.

following the findings on [11, 25, 13], in this project we will study the PNJL model, examining QCD thermodynamics at finite temperature and quark chemical potential. By analyzing the model's predictions, we can gain insights into the fundamental behaviour of matter near the Critical End Point(CEP).

Chapter 2

PNJL Model For Two Flavor Quarks

The Polyakov-Nambu-Jona-Lasinio (PNJL) model stands as a powerful theoretical framework in contemporary particle physics, offering profound insights into the non-perturbative regime of Quantum Chromodynamics (QCD)[11]. The PNJL model amalgamates two seminal concepts in theoretical physics: the Nambu-Jona-Lasinio (NJL) model and the Polyakov loop[25], each addressing distinct facets of QCD dynamics. The NJL model, a chiral effective field theory, captures the spontaneous breaking of chiral symmetry and the emergence of dynamical quark masses[14]. On the other hand, the Polyakov loop, originating from finite-temperature QCD, encapsulates the deconfinement transition and the thermodynamics of quarks and gluons at high temperatures[11, 13].

In the PNJL model, quarks interact via effective four-quark interactions resembling those in the NJL model, augmented by the inclusion of the Polyakov loop potential, which introduces temperature dependence and encodes the effects of colour confinement. The interplay between chiral symmetry restoration and deconfinement transitions manifests rich phase structures, offering insights into the QCD phase diagram under extreme conditions of temperature and density.

In this section we will do a comprehensive overview of the PNJL model, discussing its key concepts and mathematical formalism.

2.1 Polyakov Loop And Effective Potential In Pure Gauge Sector

Following [11], an effective potential of the complex Polyakov loop field provides a convenient framework for describing the deconfinement phase transition in pure $SU(N_c)$ gauge theory. To study the SU(Nc) phase structure, we need to define an appropriate order parameter. For this, we will use the Polyakov line,

$$L(\vec{x}) \equiv \mathcal{P} \exp\left[i \int_0^\beta d\tau A_4(\vec{x}, \tau)\right] \tag{2.1}$$

Here $A_4 = iA^0$ represents the temporal component of the Euclidean gauge field $(\vec{A}, A_4)$, where the strong coupling constant g_S has been absorbed. The symbol $\mathcal{P}$ denotes path ordering, and $\beta = 1/T$ is taken in the natural unit.

upon regularizing this theory on the lattice, the Polyakov loop is obtained as :

$$l(\vec{x}) = \frac{1}{N_c} \operatorname{Tr} L(\vec{x}) \tag{2.2}$$

is a color singlet under $SU\,(N_c)$, but transforms non-trivially, like a field of charge one, under $\mathbb{Z}_{N_c}$. The thermal expectation value of the Polyakov loop is used as an order parameter for the deconfinement phase transition [14].The Physical Interpretation of $\langle l(\vec{x})\rangle$ is related to the change of free energy occurring when a heavy color source in the fundamental representation is added to the system. which can be shown as:

$$\langle l(\vec{x})\rangle = e^{-\beta \Delta F_Q(\vec{x})}. \tag{2.3}$$

$\langle l(\vec{x})\rangle = 0$, in the $\mathbb{Z}_{N_c}$ symmetric phase, this implies an infinite amount of free energy is needed to add an isolated heavy quark to the system, so here phase color is confined. Now in $SU(3)$ gauge theory, the Polyakov line $L(\vec{x})$ gets replaced by its gauge

covariant averaged over a finite region of space, denoted as $\langle\langle L(\vec{x})\rangle\rangle$. The Polyakov loop[1] field:

$$\Phi(\vec{x}) \equiv \langle\langle l(\vec{x})\rangle\rangle = \frac{1}{N_c}\,\mathrm{Tr}_c\langle\langle L(\vec{x})\rangle\rangle \tag{2.4}$$

is introduced.

Following [11] from the expression(2.4), An effective potential is constructed, respecting the symmetries of the original Lagrangian and chosen to reproduce lattice calculation results at a mean field level. In this approximation, the Polyakov loop field $\Phi(\vec{x})$ is set equal to its expectation value $\Phi =$ constant, which minimizes the potential:

$$\frac{\mathcal{U}(\Phi,\bar{\Phi};T)}{T^4} = -\frac{b_2(T)}{2}\bar{\Phi}\Phi - \frac{b_3}{6}\left(\Phi^3+\bar{\Phi}^3\right) + \frac{b_4}{4}(\bar{\Phi}\Phi)^2 \tag{2.5}$$

with,

$$b_2(T) = a_0 + a_1\left(\frac{T_0}{T}\right) + a_2\left(\frac{T_0}{T}\right)^2 + a_3\left(\frac{T_0}{T}\right)^3. \tag{2.6}$$

Here, $\mathcal{U}(\Phi,\bar{\Phi};T)$ is the ansatz for the effective potential of the traced Polyakov loop Φ and its conjugate $\bar{\Phi}$, and T is the temperature.A precision fit of the parameters a_i and b_i has been performed in Ref. [25] to reproduce the Polyakov loop's expectation value using the lattice data. The results are shown in Table(2.1). Minimising the potential allows computation of pressure, entropy, and energy density. The parameter T_0 is the critical temperature for the de-confinement phase transition in pure gauge lattice theories, and from the lattice data, its value is 270 MeV.

The effective potential exhibits a phase transition from colour confinement ($T < T_0$, where the minimum is at $\Phi = 0$) to colour de-confinement ($T > T_0$, with minima

[1]the Polyakov line with periodic boundary conditions

at $\Phi \neq 0$), as illustrated in Fig.4.1a.

a_0	a_1	a_2	a_3	b_3	b_4
6.75	-1.95	2.625	-7.44	0.75	7.5

Table 2.1: Parameter for the effective potential(2.5) in the pure gauge sector.

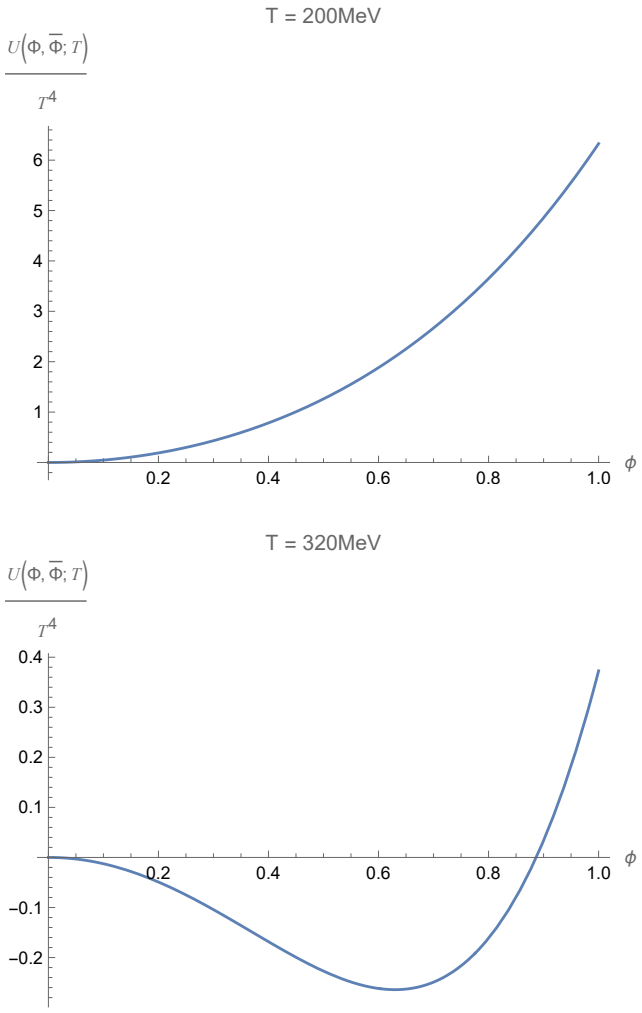

Figure 2.1: Scaled Polyakov loop effective potential $\frac{\mathcal{U}(\Phi,\bar{\Phi};T)}{T^4}$ as a function of for two values of temperature T, taking $\phi = \bar{\phi}$

.

2.2 Nambu Jona-Lasinio model

The Nambu-Jona-Lasinio (NJL) model, introduced by Yoichiro Nambu and Giovanni Jona-Lasinio in 1961 [24], is a theoretical framework in Quantum Chromodynamics (QCD) that aims to describe the phenomenon of chiral symmetry breaking. Chiral symmetry refers to the equivalence of left-handed and right-handed quarks in the absence of mass. However, in our observable universe, quarks acquire mass through their interaction with the Higgs field, breaking this symmetry.

The NJL model treats quarks as point-like particles interacting through a four-fermion interaction. This interaction generates a dynamical mass for the quarks, effectively mimicking the effect of the Higgs field. The model successfully reproduces some key aspects of chiral symmetry breaking (ref appendix A), such as the existence of a condensate of quark-antiquark pairs at low energies [19].

However, the NJL model has limitations. It doesn't incorporate confinement physics. Additionally, it struggles to accurately describe the behaviour of QCD at high temperatures and densities, where quarks and gluons become deconfined, forming a quark-gluon plasma [26].

2.2.1 Two flavours NJL model in vacuum

The NJL model operates effectively below the momentum threshold of QCD, denoted as $\Lambda_{QCD} = 0.3GeV$. At this scale, the presence of solely the three lightest quark flavours - up (u), down (d), and strange (s) - remains pertinent. For simplicity, we adopt a two-flavour NJL model, assuming equal masses for up and down quarks.

Initially, we focus solely on the scalar and pseudoscalar-isovector interaction components. The corresponding Lagrangian is represented as follows:

$$\mathcal{L}_{\mathrm{NJL}} = \bar{\psi}\left(i\gamma_\mu\partial^\mu - m_0\right)\psi + \frac{G}{2}\left[(\bar{\psi}\psi)^2 + \left(\bar{\psi}i\gamma_5\vec{\tau}\psi\right)^2\right], \tag{2.7}$$

in the above equation, $m_0 = \mathrm{diag}\,(m_u, m_d)$ with $m_u = m_d \equiv m_0$ (keeping the isospin symmetry)and $\vec{\tau}$'s are $SU_f(2)$ Pauli matrices acting on the SU(2) flavour space; G is the coupling constants of local scalar type four-quark interaction. If $\hat{m} = 0$, it upholds the chiral $SU_L(2) \times SU_R(2)$ symmetry. However, when $\hat{m} \neq 0$, the chiral symmetry explicitly breaks from $SU_L(2) \times SU_R(2)$ to $SU_f(2)$, which remains exact owing to the choice of $m_u = m_d \equiv m_0$.

2.2.2 parameter fixing

The parameters outlined in Eq. (1) are typically determined to match the mass and decay constant of the pion, along with the chiral condensate. Table 2.2 presents the parameters we employ, along with the computed physical quantities utilized to determine these parameters. The Hartree quark mass, also known as the constituent quark mass, is set at $m = 325$MeV, while the pion decay constant and mass are obtained through a Hartree + RPA calculation[25].

Table 2.2: Parameter set used in the NJL model part of the effective Lagrangian (2.8), and the resulting physical quantities. we obtain a constituent quark mass $m = 325$MeV.

Λ[GeV]	G[GeV^{-2}]	m_0[MeV]
0.651	10.08	5.5
$\left\lvert\langle\bar{\psi}_u\psi_u\rangle\right\rvert^{1/3}$ [MeV]	f_π[MeV]	m_π[MeV]
251	92.3	139.3

2.3 Coupling between quarks and the gauge sector

The Polyakov-Nambu-Jona-Lasinio (PNJL) model aims to succinctly capture two key phenomena in Quantum Chromodynamics (QCD): namely deconfinement and chiral symmetry breaking. To account for the coupling between light quarks and the chiral condensate $\langle\bar{\psi}\psi\rangle$ (order parameter for the chiral symmetry), we begin with a two-flavour Nambu-Jona-Lasinio (NJL) description of quarks(globally $SU_c(3)$ symmetric and chirally invariant point-like interaction). The quarks are then minimally coupled to the Polyakov loop through the Lagrangian [4]:

$$\mathcal{L}_{PNJL} = \bar{\psi}\left(i\gamma_\mu D^\mu - \hat{m}_0\right)\psi + G\left[(\bar{\psi}\psi)^2 + \left(\bar{\psi}i\gamma_5\vec{\tau}\psi\right)^2\right] - \mathcal{U}(\Phi,\bar{\Phi};T), \tag{2.8}$$

Here, $\psi = (\psi_u, \psi_d)$ denotes the quark fields and the covariant derivative $D^\mu = \partial^\mu - iA^\mu$The gauge coupling g is absorbed in the definition of $A^\mu(x) = g\mathcal{A}^\mu_a(x)\frac{\lambda_a}{2}$ where $\mathcal{A}^\mu_a$ is the SU(3) gauge field and λ_a are the Gell-Mann matrices. The two flavours current quark mass matrix is $\hat{m}_0 = \mathrm{diag}(m_u, m_d)$, we will be working in isospin symmetry limits with $m_u = m_d \equiv m_0$. The parameter G characterizes the coupling strength of the chirally symmetric scalar-pseudoscalar four-point interaction of the quark fields. In [25], using the Matsubara formalism consider the isospin symmetric case(thus not including the iso-spin chemical potential,μ_I), with an equal number of u and d quarks (and therefore a single quark chemical potential,μ). the expression for thermodynamic potential per unit volume at finite temperature is calculated to be:

$$\begin{aligned}\Omega_{PNJL} =& \mathcal{U}(\Phi,\bar{\Phi},T) + \frac{\sigma^2}{2G} - 2N_f T \\ &\times \int \frac{\mathrm{d}^3p}{(2\pi)^3}(\ln\left[1 + 3\left(\Phi + \bar{\Phi}\mathrm{e}^{-(E_p-\mu)/T}\right)\mathrm{e}^{-(E_p-\mu)/T} + \mathrm{e}^{-3(E_p-\mu)/T}\right] \\ &+ \ln\left[1 + 3\left(\bar{\Phi} + \Phi\mathrm{e}^{-(E_p+\mu)/T}\right) \times \mathrm{e}^{-(E_p+\mu)/T} + \mathrm{e}^{-3(E_p+\mu)/T}\right]) \\ &- 6N_f \int \frac{\mathrm{d}^3p}{(2\pi)^3} E_p\theta\left(\Lambda^2 - \vec{p}^2\right)\end{aligned} \tag{2.9}$$

where we have introduced the quark quasiparticle energy $E_p = \sqrt{\vec{p}^2 + m^2}$, m = $m_0 - \langle\sigma\rangle = m_0 - G\langle\bar{\psi}\psi\rangle$, The last term involves the NJL three-momentum cutoff Λ, to remove Ulra violet deviation by hard regularization . The second term doesn't require any cutoff since the coupled Fermi-Dirac function prevents the term from diverging. The value of the parameters G,m_0 and Λ are calculated in [25], which is summarised in (2.2). This model is expected to work up to an upper limit of temperature Since the gluon physics is contained only in a static background field in the Polyakov loop. The transverse degrees of freedom will become relevant for $T > 2.5T_c$ [22].

Chapter 3

Formalism

Here we will outline the methodologies used to derive the Cross over Temperature and various thermodynamic quantities using the PNJL model.

3.1 The Mean Fields And Cross Over Temperature

The equations of motion for the mean fields Φ, $\bar{\Phi}$, and σ are derived from Ω_{PNJL} using:

$$\frac{\partial\Omega}{\partial\sigma} = 0, \quad \frac{\partial\Omega}{\partial\Phi} = 0, \quad \frac{\partial\Omega}{\partial\bar{\Phi}} = 0. \tag{3.1}$$

This set of coupled equations is then solved for the mean fields as functions of temperature T and quark chemical potential μ. The values of the fields obtained can then be used to evaluate all the thermodynamic quantities in the mean-field approximation. To obtain the transition point we need to look at the temperature derivatives of the fields.

To evaluate the cross over Temperature. First, Equation. (3.1) is solved numerically for each value of temperature T at $\mu_0 = 0$. Then the slope of the $(T, \Phi(T))$ and the $(T, \sigma(T))$ curves is calculated using the deferential Method. The Peak of the (T,$\partial\Phi/\partial T$) gives us the deconfinement Temperature and The Peak of the (T, $\partial\sigma/\partial T$) gives us the chiral Temperature. The crossover temperature is calculated as mean of deconfinement and chiral Temperatures.

3.2 Taylor expansion of pressure

The expression of pressure as a function of temperature T and baryon chemical potential μ_0 is denoted as:

$$P\left(T,\mu_0\right) = -\Omega\left(T,\mu_0\right). \tag{3.2}$$

On the lattice, the direct simulation for nonzero μ_0 (baryon chemical potential) is not possible, the Quark Number Susceptibility (QNS) and higher-order derivatives (HODs) computed at $\mu_0 = 0$ are utilized as Taylor expansion coefficients. This is done to extract the chemical potential dependence of pressure. the convergence of such an expansion has been assessed using the HODs to obtain the Critical End Point(CEP).

In our work the Ω_{PNJL} is used to obtain pressure from (3.2). We can then expand the scaled pressure as:

$$\frac{P\left(T,\mu_0\right)}{T^4} = \sum_{n=0}^{\infty} c_n(T)\left(\frac{\mu_0}{T}\right)^n, \tag{3.3}$$

using Taylor series expansion, where

$$c_n(T) = \frac{1}{n!}\frac{\partial^n\left(P\left(T,\mu_0\right)/T^4\right)}{\partial\left(\frac{\mu_0}{T}\right)^n}\bigg|_{\mu_0=0}. \tag{3.4}$$

We will use the expansion around $\mu_0 = 0$. In this expansion, the odd terms vanish due to CP symmetry[1]. We extract the expansion coefficients up to the eighth order by using 3.4 and then use the field values that are obtained from the equation. (3.1) to find the there values at each Temperature.[2]

[1] We can also see this by expanding terms in Ω_{PNJL}.

[2] This has been motivated by the fact that on the lattice the most recent results are also obtained up to this order.

3.2.1 C_V, v_s^2, and $\mathcal{C}$

The energy density ϵ is derived from the thermodynamic potential Ω through the equation:

$$\epsilon = -T^2 \frac{\partial(\Omega/T)}{\partial T}\bigg|_V = -T\frac{\partial \Omega}{\partial T}\bigg|_V + \Omega. \tag{3.5}$$

he rate of change of energy density ϵ with temperature at constant volume is the specific heat C_V , is expressed as:

$$C_V = \frac{\partial \epsilon}{\partial T}\bigg|_V = -T\frac{\partial^2 \Omega}{\partial T^2}\bigg|_V . \tag{3.6}$$

In the case of a continuous phase transition, we anticipate a divergence in C_V, which corresponds to significantly enhanced transverse momentum fluctuations or highly suppressed temperature fluctuations. This is particularly relevant if the dynamics in relativistic heavy-ion collisions position the system in close proximity to the Critical End Point (CEP).

The square of the velocity of sound at constant entropy S is defined as:

$$v_s^2 = \frac{\partial P}{\partial \epsilon}\bigg|_S = \frac{\partial P}{\partial T}\bigg|_V \Big/ \frac{\partial \epsilon}{\partial T}\bigg|_V = \frac{\partial \Omega}{\partial T}\bigg|_V \Big/ T\frac{\partial^2 \Omega}{\partial T^2}\bigg|_V \tag{3.7}$$

Given that the denominator corresponds to C_V, a divergence in the specific heat implies that the velocity of sound goes to zero at the CEP.

The conformal measure $\mathcal{C}$ is defined as

$$\mathcal{C} = \frac{\Delta}{\epsilon} = \frac{\epsilon - 3P}{\epsilon} \simeq 1 - 3v_s^2. \tag{3.8}$$

Thus, a minimum in the velocity of sound, as expected near a phase transition or crossover, correspond to a maximum in $\mathcal{C}$. Considering the last relation, it is evident that at asymptotic temperatures where v_s^2 approaches the ideal gas value of 1/3, the conformal measure tends towards the conformal limit $\mathcal{C} = 0$.

Chapter 4

Results

4.1 Numerical Solution for the mean fields in finite temperature and zero chemical potential

The solutions of the mean field equations 3.1 are :

$$\begin{aligned}
\frac{\partial\Omega}{\partial\Phi} =&0 \\
=&\frac{T^4}{2}\left(-b_2(T)\bar{\Phi} - b_3\Phi^2 + b_4\Phi\bar{\Phi}^2\right) \\
&- 6N_fT\int_\Lambda \frac{\mathrm{d}^3p}{(2\pi)^3}\left\{\frac{e^{-2(E_p-\mu)/T}}{1+3\left(\bar{\Phi}+\Phi e^{-(E_p-\mu)/T}\right)e^{-(E_p-\mu)/T}+e^{-3(E_p-\mu)/T}}\right. \\
&\left.+\frac{e^{-(E_p+\mu)/T}}{1+3\left(\Phi+\bar{\Phi}e^{-(E_p+\mu)/T}\right)e^{-(E_p+\mu)/T}+e^{-3(E_p+\mu)/T}}\right\}
\end{aligned} \tag{4.1}$$

$$\begin{aligned}
\frac{\partial\Omega}{\partial\bar{\Phi}} =&0 \\
=&\frac{T^4}{2}\left(-b_2(T)\Phi - b_3\bar{\Phi}^2 + b_4\bar{\Phi}\Phi^2\right) \\
&- 6N_fT\int_\Lambda \frac{\mathrm{d}^3p}{(2\pi)^3}\left\{\frac{e^{-(E_p-\mu)/T}}{1+3\left(\bar{\Phi}+\Phi e^{-(E_p-\mu)/T}\right)e^{-(E_p-\mu)/T}+e^{-3(E_p-\mu)/T}}\right. \\
&\left.+\frac{e^{-2(E_p+\mu)/T}}{1+3\left(\Phi+\bar{\Phi}e^{-(E_p+\mu)/T}\right)e^{-(E_p+\mu)/T}+e^{-3(E_p+\mu)/T}}\right\}
\end{aligned} \tag{4.2}$$

$$\frac{\partial\Omega}{\partial\sigma} =0 \tag{4.3}$$

In Figure (4.1a), we have numerically solved for 3.1 and obtained the behaviour of Scaled chiral condensate and Polyakov loop Φ as a temperature at $\mu = 0$, where we find $\Phi = \bar{\Phi}$.

Introducing quarks coupled to the σ and Φ fields transforms the initial first-order transition observed in pure-gauge Lattice QCD into a continuous crossover. The

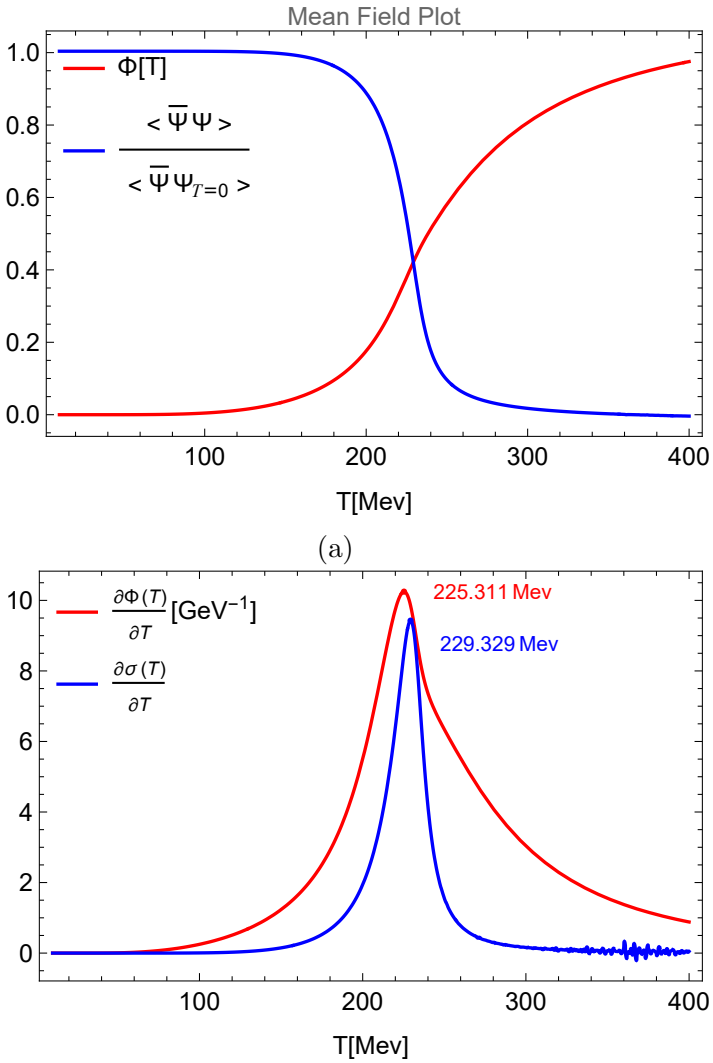

Figure 4.1: (a): scaled chiral condensate and Polyakov loop Φ as functions of temperature at zero chemical potential. (b): plots of $\partial\sigma(T)/\partial T$ and $\partial\Phi(T)/\partial T$.

pure-gauge system displays a first-order transition at the critical temperature $T_0 = 270$MeV. However, once quarks are introduced, the crossover transitions for the chiral condensate $\langle\bar{\psi}\psi\rangle$ and the Polyakov loop coincide at a lower critical temperature $T_c \simeq 229$MeV (refer to Fig. (4.1b)). This shift in transition occurs without any alterations to the parameters from the pure-gauge scenario. Our results are identical to that obtained in Ref. [25].

The obtained critical temperature slightly exceeds the data available for two-flavor Lattice QCD [15, 16], which suggests $T_c = (173 \pm 8)$MeV. To align with existing lattice findings, we opt to decrease T_c by adjusting the parameter T_0 from 270 to 190MeV[25]. By defining T_c in this scenario as the mean of the two transition temperatures, we derive $T_c \simeq 182$MeV(refer figure. (4.2)), which aligns with the findings in [7].

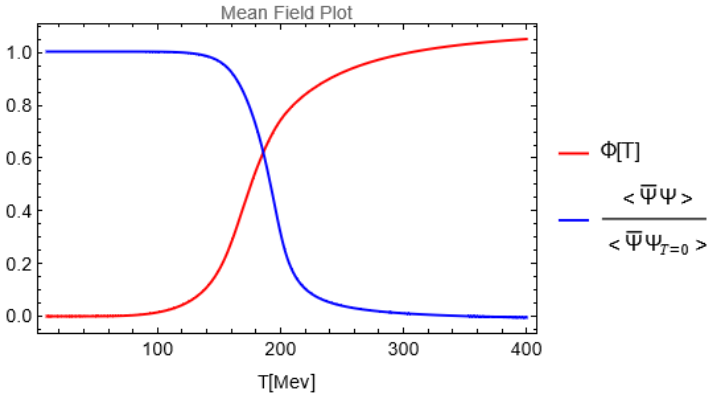

(a)

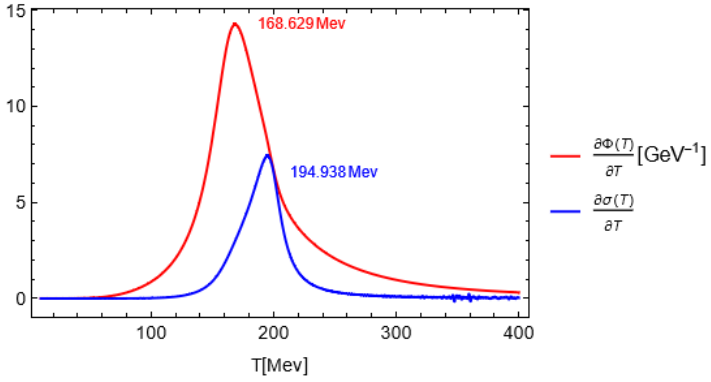

(b)

Figure 4.2: The numerical Solution of (3.1) by taking $T_0 = 190MeV$. (a): scaled chiral condensate and Polyakov loop Φ as functions of temperature at zero chemical potential. (b): plots of $\partial\sigma(T)/\partial T$ and $\partial\Phi(T)/\partial T$.

4.2 Taylor expansion of pressure

In Figure 4.3, the pressure scaled with the Stefan-Boltzmann pressure (P/P_{SB} for an ideal gas) is plotted as a function of T/T_c. Up to $2.5T_c$, the pressure rises from

nearly zero at low temperatures to approximately 90% of its ideal gas value. This value is somewhat elevated compared to continuum estimates obtained from lattice calculations (Karsch et al., 2000)[17], which yield around 80% of P_{SB}.

A comparison between our findings and the PNJL model results presented in Fig. 7a of Ref[25], reveals a striking resemblance, even though there is a noticeable discrepancy in the choice of T_0, with our measurement indicating $T_0 = 270$ MeV as opposed to their reported value of $T_0 = 190$ MeV.

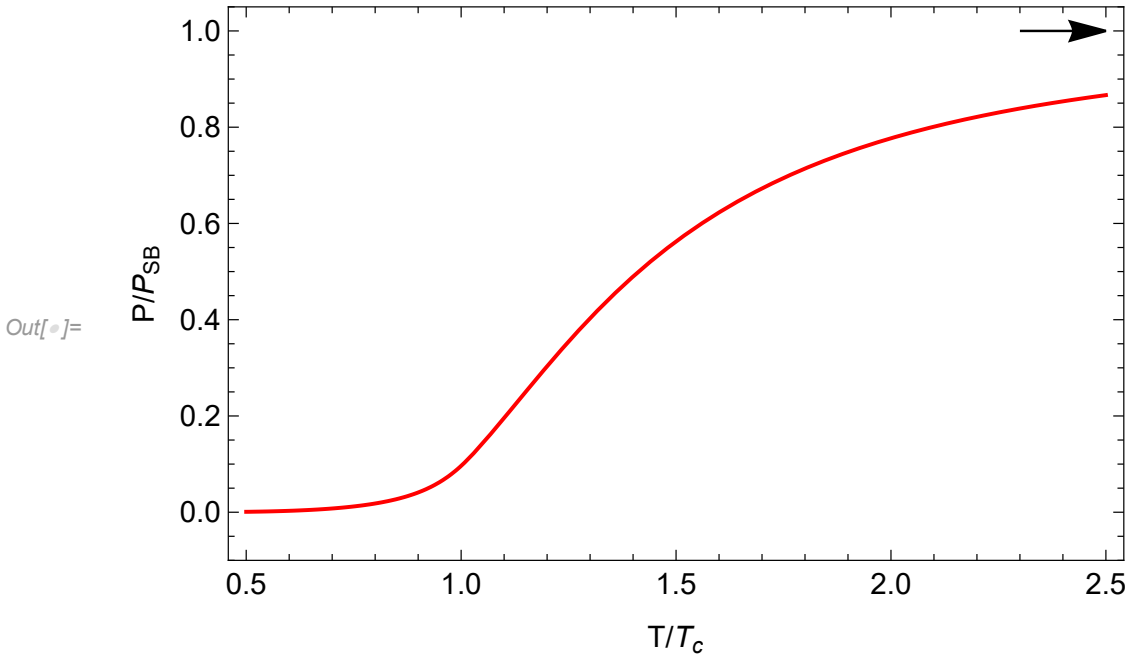

Figure 4.3: pressure scaled with the Stefan-Boltzmann pressure as a function of temperature in the PNJL model, at $\mu = 0$. The arrow on the right indicates the ideal gas value.

Now, we compute the derivatives of pressure with respect to μ at $\mu = 0$, using Equation 3.4. Figure 4.4 depicts the variation of the quark number susceptibility (QNS), denoted as c_2, with respect to T/T_c. Notably, this plot exhibits behaviour reminiscent of an order parameter.

In Figure (4.5), we calculated the fourth-order derivative, c_4, also known as the sus-

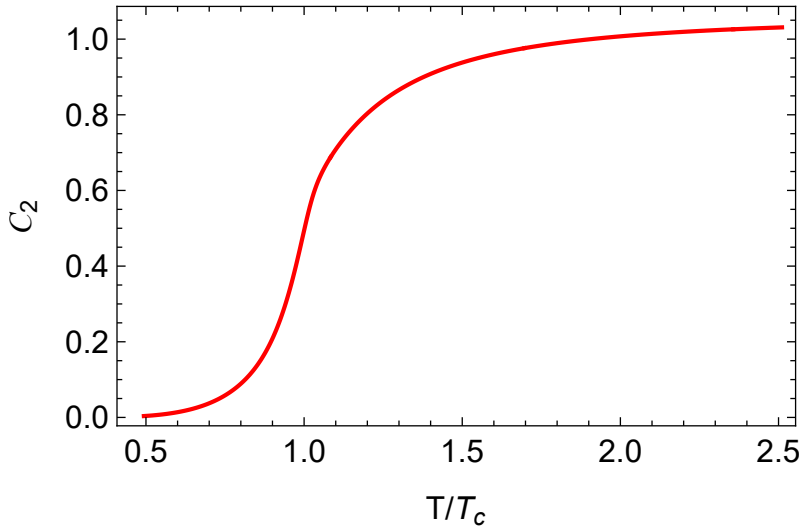

Figure 4.4: The QNS as a function of T/T_c.

ceptibility of c_2. c_4 converges to the Stefan-Boltzmann (SB) limit as the temperature approaches T_c. However, it's worth noting a substantial deviation from the findings of Allton et al. (2005)[5]and [13], where c_4 exhibits a spike near T_c before converging to twice the SB limit.

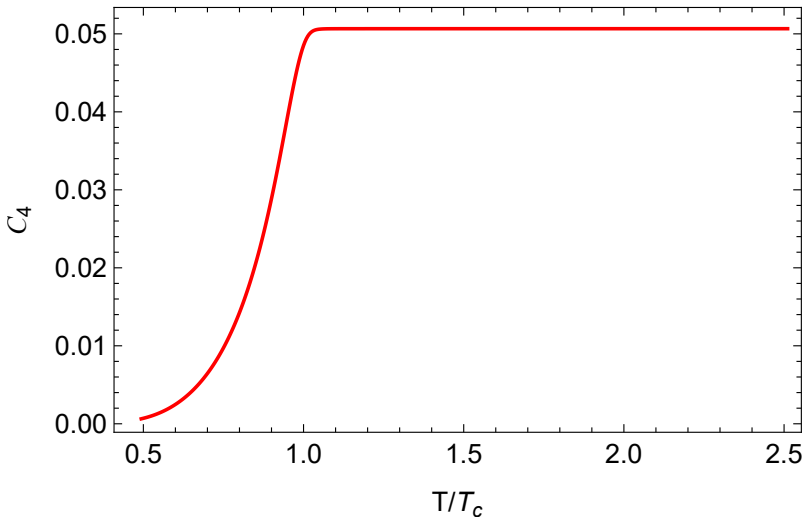

Figure 4.5: The c4 as a function of T/T_c.

In Figures 4.6 and 4.7, we present the higher-order derivatives, c_6 and c_8, respectively. Notably, at high temperatures, both of these higher-order derivatives converge to zero. However, the structure near T_c is particularly intriguing. Our results exhibit substantial deviations from those reported in previous studies by Ghosh et al. (2006)[13] and Allton et al. (2005)[5].

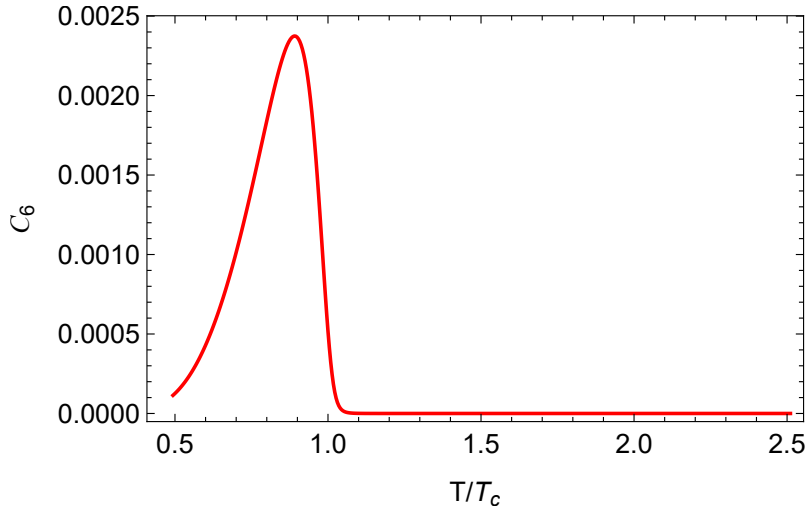

Figure 4.6: The c_6 as a function of T/T_c.

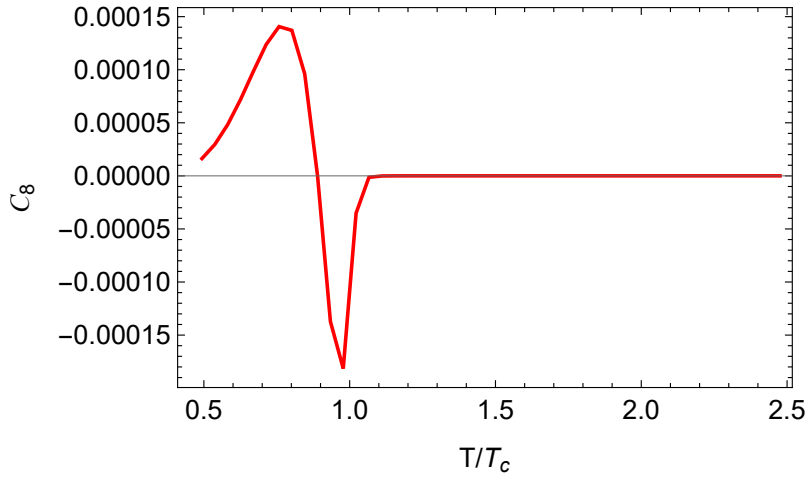

Figure 4.7: The c_8 as a function of T/T_c from the PNJL model

4.3 C_V, v_s^2, and $\mathcal{C}$

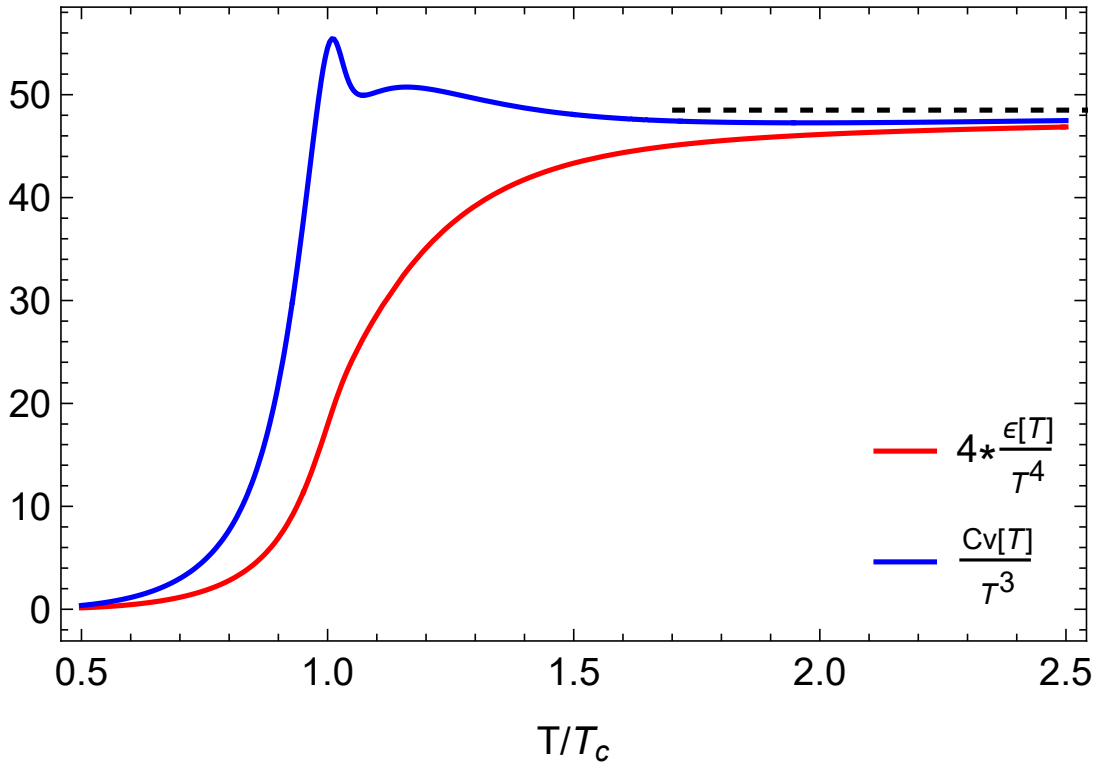

Figure 4.8: C_V/T^3 and $4\epsilon/T^4$ as a function of T/T_c. The dashed line on the right shows the ideal gas value.

We will now analyse the other Computed thermodynamic quantities at finite temperatures and $\mu = 0$. The specific heat, as shown in Fig.4.8, increases with the temperature, peaking at T_c. Subsequently, it experiences a rapid decline over a narrow temperature range. Following this, a broad yet subtle bump is observed around $T = 270$MeV, gradually approaching a value slightly below that of the ideal gas. Upon comparison with lattice data for pure glue theory (Fig.3f, Ref[12]), it becomes apparent that the deviation from the ideal gas value is notably smaller in our case. Additionally, we have included a plot of $4\epsilon/T^4$, where the specific heat is expected to coincide for a conformal gas. We can see that the values of C_v/T^3 and $4\epsilon/T^4$ are almost equal at the large temperatures.

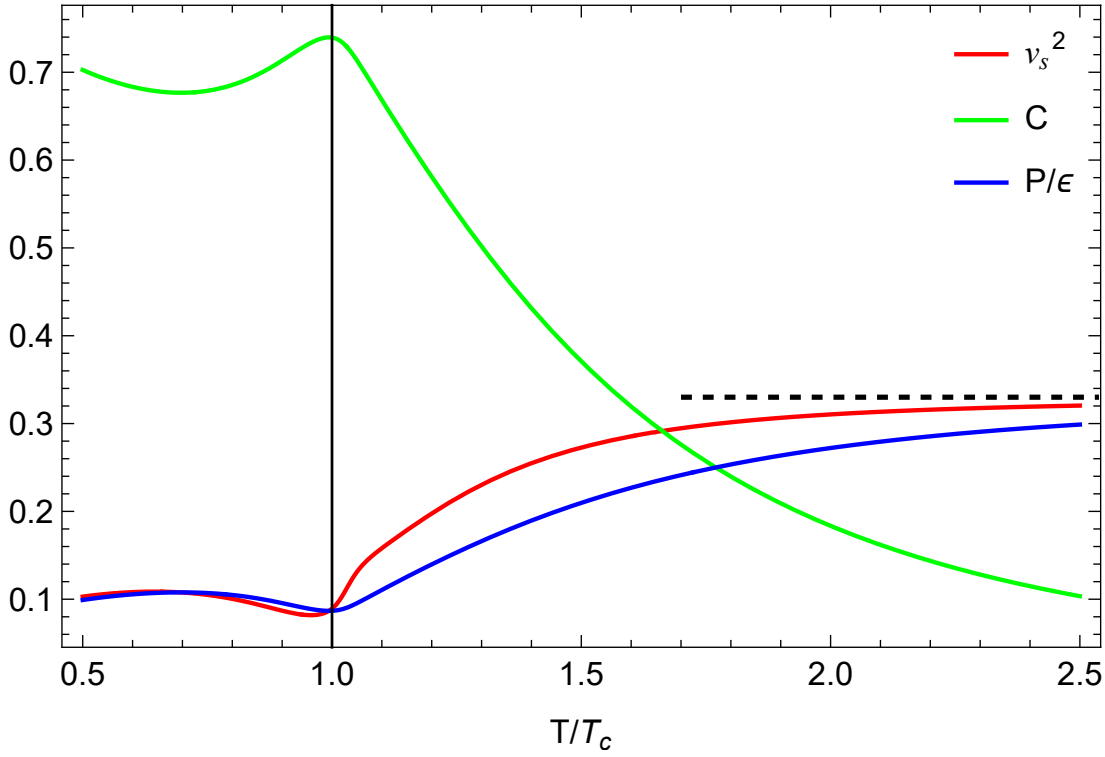

Figure 4.9: Squared velocity of sound v_s^2 and conformal measure $\mathcal{C} = \Delta/\epsilon$ as a function of T/T_c . The dashed line on the right shows the ideal gas value for v_s^2. For comparison with v_s^2 we also plot the ratio P/ϵ .

In the figure(4.9), we have plotted v_s^2 and $\mathcal{C}$. As expected from the relation.(3.8) it is clear form the plot that the two quantities(v_s^2,$\mathcal{C}$) behave in a correlated manner. It is worthwhile to note here that $\mathcal{C}$ has been computed from the zeroth and first-order coefficients of $\Omega(T, \mu = 0)$, whereas v_s^2 has been measured from the first and second-order in coefficients. We have also plotted P/ϵ for comparison with v_s^2. The value of P/ϵ matches with that of v_s^2 for $T < T_c$ and also goes close again near $2.5T_c$. But in between these two limits, the v_s^2 is greater than P/ϵ. Thus, $\mathcal{C}$ would go to zero much faster if we replace P/ϵ by v_s^2 for computing $\mathcal{C}$.

v_s^2 is close to its ideal gas value at temperatures above $2.5T_c$. This is close to the

results from pure gluon theory on the lattice as reported in Ref. [12] and also that with 2 flavour Wilson Fermions in Ref .[18]. This observation refers to the fact that v_s^2 is predominantly influenced by the gluonic degrees of freedom at high temperatures. However, in the vicinity of T_c, v_s^2 approaches a minimum value near 0.082, consistent with simulation results involving dynamical quarks in Refs.[4, 6], and notably close to the softest point $P/\epsilon = 0.075$ outlined in Ref.[8]. This is expected since the scalar σ plays a crucial role in chiral dynamics for minor quark masses.

The conformal measure C values are also consistent with the Lattice data of Ref.[12]. A slight deviation is observed near T_c where our findings range from 0.7 to 0.75, compared to the range of 0.6 to 0.7 reported for pure glue theory. However, note that the dip at temperatures less than T_c is prominent in both cases. Furthermore, at lower temperatures, we observe an increase in conformal measure. For non-relativistic ideal gas, the ratio of P/ϵ tends towards zero, leading to a convergence of C towards 1. Hence, such an increase at lower temperatures is expected. But at higher temperatures, the system should exhibit either an ideal gas or conformal behaviour, resulting in C going to zero. Our findings closely resemble the outcomes from pure gauge Lattice results in this regard.

Chapter 5

Summary and Conclusions

In this study, we investigated the Polyakov loop extended Nambu Jona-Lasinio (PNJL) model in capturing the fundamental aspects of QCD thermodynamics, including deconfinement and chiral symmetry, under finite temperature and nonzero quark chemical potential conditions. In the mean-field approximation, Utilizing the minimization condition(3.1) on the thermodynamic chemical potential, we derived expressions for the scaled chiral condensate and Polyakov loop field, which allowed us to analyze their behaviour as functions of temperature and chemical potential.

We have reproduced the mean fields as a function of temperature at vanishing chemical potential successfully in figure (4.1a), our analysis of the temperature derivatives of the mean fields (ref 4.1b) revealed a significant peak in both the chiral condensate and Polyakov loop derivatives near Critical End Point(CEP), obtaining an effective cross-over temperature of $T_c = 227MeV$, consistent with previous estimates in [13, 25]. Furthermore, employing the mean-field values obtained, we computed the thermodynamic pressure (ref 4.3) as a function of temperature and performed a Taylor Series Expansion to extract coefficients.

We've computed the specific heat (refer. (4.8)), speed of sound(refer. (4.9))and conformal measure at finite temperature and $\mu = 0$, and these results closely match Lattice data[12]. At high temperatures, gluonic contributions appear to dominate the system's behaviour. Around the cross-over temperature, meaningful differences emerge between Lattice data for pure QCD and that with dynamical quarks.Our results suggest that simulations incorporating dynamical quarks provide a more ac-

curate representation of the system's behavior in this temperature regime.

5.1 Future Prospects

Looking ahead, while the PNJL model has demonstrated considerable success in elucidating various facets of strongly interacting matter, notable challenges remain. Future research efforts should focus on refining the model to incorporate dynamic effects beyond mean-field approximations, such as fluctuations and correlations, particularly near phase boundaries. Additionally, extending the PNJL model to finite baryon chemical potentials presents an exciting avenue for exploration, with potential implications for experiments at facilities like the Relativistic Heavy Ion Collider (RHIC) and the Large Hadron Collider (LHC). These endeavors hold promise for advancing our understanding of the QCD phase diagram and the behavior of strongly interacting matter in extreme conditions.

References

[1] Effective field theories. 43(1), 1995.

[2] *World scientific lecture notes in physics*, volume 50. World Scientific Publishing Company, 1998.

[3] C. Alcock and E. Olinto. The proto-neutron star interior and quark deconfinement. 294, 1985.

[4] A. Ali Khan and et al. Chiral dynamics in $N_f = 2$ lattice qcd with multiple masses. *Physical Review D*, 64:074510, 2001.

[5] CR Allton, M Döring, S Ejiri, SJ Hands, Olaf Kaczmarek, Frithjof Karsch, Edwin Laermann, and K Redlich. Thermodynamics of two flavor qcd to sixth order in quark chemical potential. *Physical Review D*, 71(5):054508, 2005.

[6] Y. Aoki, Z. Fodor, S. D. Katz, and K. K. Szabo. The equation of state in lattice qcd: With physical quark masses towards the continuum limit. *Journal of High Energy Physics*, 2006(1):089, 2006.

[7] S. Digal, E. Laermann, and H. Satz. Title of the third paper. *European Physical Journal C*, 18:583, 2001.

[8] S. Ejiri, F. Karsch, E. Laermann, and C. Schmidt. Lattice qcd at non-zero temperature and density. *arXiv preprint hep-lat/0512040*, 2005.

[9] F. Carminati et al. Alice: Physics performance report, volume i. 30, 2004.

[10] K. Adcox et al. Formation of dense partonic matter in relativistic nucleus-nucleus collisions at rhic: Experimental evaluation by the phenix collaboration. 757, 2005.

[11] Kenji Fukushima. Chiral effective model with the polyakov loop. *Physics Letters B*, 591(3-4):277–284, 2004.

[12] Rajiv V Gavai, Sourendu Gupta, and Swagato Mukherjee. Lattice qcd equation of state: improving the differential method. *arXiv preprint hep-lat/0506015*, 2005.

[13] Sanjay K Ghosh, Tamal K Mukherjee, Munshi G Mustafa, and Rajarshi Ray. Susceptibilities and speed of sound from the polyakov-nambu-jona-lasinio model. *Physical Review D*, 73(11):114007, 2006.

[14] Hubert Hansen, Wanda Maria Alberico, Andrea Beraudo, Alfredo Molinari, Marzia Nardi, and C Ratti. Mesonic correlation functions at finite temperature and density in the nambu–jona-lasinio model with a polyakov loop. *Physical Review D*, 75(6):065004, 2007.

[15] F. Karsch. Title of the first paper. *Lecture Notes in Physics*, 583:209, 2002.

[16] F. Karsch, E. Laermann, and A. Peikert. Title of the second paper. *Nuclear Physics B*, 605:579, 2002.

[17] Frithjof Karsch, Edwin Laermann, and A Peikert. The pressure in 2, 2+ 1 and 3 flavour qcd. *Physics Letters B*, 478(4):447–455, 2000.

[18] A Ali Khan, S Aoki, R Burkhalter, S Ejiri, M Fukugita, S Hashimoto, N Ishizuka, Y Iwasaki, K Kanaya, T Kaneko, et al. Equation of state in finite-temperature

qcd with two flavors of improved wilson quarks. *Physical review D*, 64(7):074510, 2001.

[19] S. P. Klevansky, R. Rapp, and T. Schafer. *Chiral perturbation theory in Minkowski space*, volume 454 of *Lecture Notes in Physics*. Springer, 2008.

[20] J. Madsen. The phases of matter in neutron stars. 63(4), 2009.

[21] P. Maris and goprojected [USQCD Collaboration]. Glueball mass from lattice qcd. 79(24), 1997.

[22] Peter N Meisinger, Michael C Ogilvie, and Travis R Miller. Gluon quasiparticles and the polyakov loop. *Physics Letters B*, 585(1-2):149–154, 2004.

[23] Tamal Kr Mukherjee, Sanjay K Ghosh, Munshi G Mustafa, and Rajarshi Ray. Susceptibilities and speed of sound from pnjl model. 2006.

[24] Yoichiro Nambu and Giovanni Jona-Lasinio. Dynamical model of elementary particles based on an analogy with superconductivity. *Physical Review*, 122(1):345–358, 1961.

[25] Claudia Ratti, Michael A Thaler, and Wolfram Weise. Phases of qcd: Lattice thermodynamics and a field theoretical model. *Physical Review D*, 73(1):014019, 2006.

[26] M. A. Stephanov. Qcd phase diagram and the limits of perturbative calculations. *Progress in Theoretical Physics Supplement*, 186:348–363, 2010.

Appendix A

Chiral Symmetry Breaking

A significant aspect tied to the QCD Lagrangian revolves around chiral symmetry. Quarks are categorized based on their chirality: right (where spin and momentum align) and left (where they oppose each other). We denote ψ_R as the field for "right quarks" and ψ_L for "left quarks," which can be represented as:

$$\psi = \begin{pmatrix} \psi_R \\ \psi_L \end{pmatrix}. \tag{5.1}$$

Using the γ^5 matrix defined in a Weyl (chiral) representation:

$$\gamma^5 = \begin{bmatrix} 1_2 & \\ & -1_2 \end{bmatrix} \tag{5.2}$$

we define the projectors upon the left and right states [20]:

$$\begin{aligned} \psi_L &= \frac{1_4 - \gamma^5}{2}\psi, & \bar{\psi_L} &= \psi_L^+\gamma_0 = \bar{\psi}\frac{1_4 + \gamma^5}{2}, \\ \psi_R &= \frac{1_4 + \gamma^5}{2}\psi, & \bar{\psi_R} &= \psi_R^+\gamma_0 = \bar{\psi}\frac{1_4 - \gamma^5}{2}, \end{aligned}$$

where 1_2 and 1_4 are respectively the 2×2 and 4×4 identity matrices. If we use these projectors in the QCD Lagrangian, and if we do not explicitly mention the flavours, we obtain:

$$\mathcal{L}_{QCD} = -\frac{1}{4} \cdot G^a_{\mu v} \cdot G^{\mu v}_a + i\bar{\psi}_R\gamma^\mu D_\mu\psi_R + i\bar{\psi}_L\gamma^\mu D_\mu\psi_L - m \cdot \bar{\psi}\psi \tag{5.3}$$

using the anti-commutation relation $\{\gamma^\mu, \gamma^5\} = 0$. The terms $i\bar{\psi}_R\gamma^\mu D_\mu\psi_R$ and $i\bar{\psi}_L\gamma^\mu D_\mu\psi_L$ shows that left quarks only interact with other left quarks, and likewise for right quarks. This segregation of left and right quarks embodies chiral symmetry. However, the term $m \cdot \bar{\psi}\psi = m \cdot \left(\bar{\psi}_R\psi_L + \bar{\psi}_L\psi_R\right)$ disrupts this symmetry because it

allows interaction between the left and right quarks, where m denotes the quark mass. Quark masses approximate their bare masses m_0 at high temperatures and densities. For quarks u and d, these bare masses are low enough to neglect the $m_0 \cdot \bar{\psi}\psi$ term, indicating an approximate chiral symmetry. This is known as explicit chiral symmetry breaking.

Now, at low temperatures and/or densities, quark-antiquark condensates may form, conventionally denoted as $\langle\langle \bar{\psi}_f \psi_f \rangle\rangle$, often referred to as quark or chiral condensates. An antiquark from a condensate can interact with a quark outside the condensate, resulting in a left quark and a condensate yielding a right quark. This interaction breaks chiral symmetry.This interaction leads to the consideration of effective quark masses. We consider there a mass m largely greater than the bare mass. The term $m \cdot \bar{\psi}\psi$ is responsible for the breaking of the chiral symmetry, thus an increase of m allows this term to become non-negligible. In this case, the chiral symmetry is spontaneously broken.